iScience

Article

# The tuna keel is a mechanosensory structure

## Graphical abstract

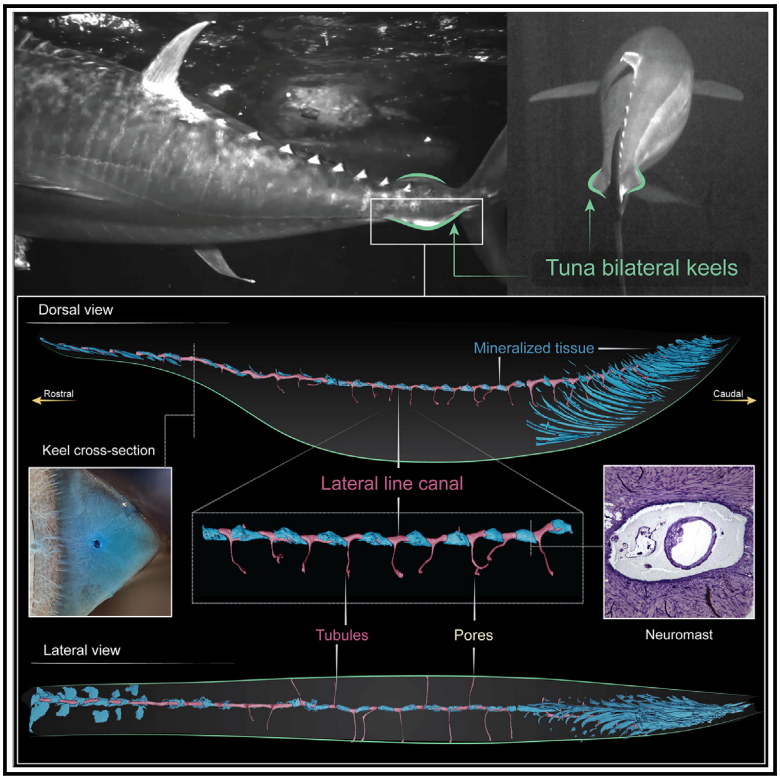


## Highlights

- The bilateral keels of yellowfin and bigeye tuna contain a novel lateral line canal
- The keel lateral line system differs in structure from the trunk lateral line system
- Keel lateral line canal contains tubules extending to the dorsal and ventral surfaces
- The keel lateral line system may measure pressure near the tail during locomotion

## Authors

Júlia Chaumel, Dylan K. Wainwright, Jacqueline F. Webb, Connor F. White, George V. Lauder

## Correspondence

julia_chaumelcerda@fas.harvard.edu

## In brief

Piscine anatomy; Zoology; Evolutionary biology

Chaumel et al., 2025, iScience *28*, 111578
January 17, 2025 
https://doi.org/10.1016/j.isci.2024.111578

CellPress

iScience

CellPress
OPEN ACCESS

Article

# The tuna keel is a mechanosensory structure

Júlia Chaumel,[1,4,5,6,*] Dylan K. Wainwright,[2,4] Jacqueline F. Webb,[3,4] Connor F. White,[1] and George V. Lauder[1]
[1]Museum of Comparative Zoology, Harvard University, Cambridge, MA 02138, USA
[2]Department of Biological Sciences, Lilly Hall of Life Sciences, 915 Mitch Daniels Boulevard, Purdue University, West Lafayette, IN 47907-2054, USA
[3]Department of Biological Sciences, University of Rhode Island, Kingston, RI 02881, USA
[4]These authors contributed equally
[5]X (formerly Twitter): @Yuliachaumel
[6]Lead contact
*Correspondence: julia_chaumelcerda@fas.harvard.edu
https://doi.org/10.1016/j.isci.2024.111578

## SUMMARY

Tunas are high-performance pelagic fishes of considerable economic importance and have a suite of biological adaptations for high-speed locomotion. In contrast to our understanding of tuna body and muscle function, mechanosensory systems of tuna are poorly understood. Here we present the discovery of a remarkable sensory lateral line canal within the bilateral tuna keels with tubules that extend to the upper and lower keel surfaces. Neuromast mechanoreceptor organs are found periodically along the canal lumen, enclosed within tubular ossifications surrounding the canal that we interpret as modified lateral line scales. In addition, a series of segmental, elongated skeletal elements of unknown homology support the posterior end of the keel. These observations suggest that the bilateral tuna keels act as flow sensing structures, perhaps providing information on tail beat frequency, amplitude, force, and water flow dynamics over the caudal region of the tuna body axis during locomotion.

## INTRODUCTION

Tunas are highly specialized fishes known for their locomotor performance and pelagic lifestyle.[1–4] Some tuna species undertake long-distance migrations of thousands of kilometers, crossing the Pacific and Atlantic Oceans multiple times to reach spawning areas and track food supplies.[1,5–9] Although long-distance migratory locomotion is typically accomplished at speeds of 0.5–1.0 body lengths per second, tunas can also accelerate rapidly and exhibit impressive locomotor maneuverability when schooling and feeding.[10–13] Tunas have also been used as models for robotic systems to study acceleration and high-performance locomotion.[3,14,15]

Morphological features of tunas that facilitate prolonged and rapid swimming include body streamlining,[2,3] the lunate tail,[2,15] cardiovascular specializations,[16–18] specialized locomotor musculature and tendons, and a narrow caudal peduncle with finlets and bilateral keels.[4,19–22] One of the key morphological specializations of tunas is the presence of a pair of keels, structures that project laterally from both sides of the caudal peduncle, rostral to the lunate tail (Figures 1A–1D; Videos S1 and S2). In tunas, swimming movements are generated by both the body and tail[3,23,24] and locomotor kinematics involve the rapid lateral displacement of the caudal region, which includes the caudal peduncle, bilateral keels, and caudal fin (Figures 1C–1E; Videos S1 and S2). Tuna keels have been studied previously with a focus on their biomechanical function during locomotion, with the aim of understanding how keel-like structures anterior to the tail could reduce recoil forces and thus improve locomotor efficiency.[4,21]

In contrast to our understanding of tuna body and muscle function, the sensory systems of tuna are poorly understood. In most species of fishes studied, the trunk canal of the lateral line system extends along the body and is defined by a tubular lateral line canal containing innervated neuromasts that respond to fluid movement within the canal.[25,26] Periodic openings of the canal to the skin surface transmit ambient fluid movement into the canal, deforming sensory hair cells that comprise the neuromast.[27,28] The lateral line systems of high-speed pelagic fishes such as tuna could differ from those of most ray-finned fishes and elasmobranchs due to the high-frequency movements involved in tuna propulsion and maneuvering.[26,29,30] The tuna lateral line sensory system could also play an important role in group behaviors such as schooling and spawning. Understanding the sensory environment experienced by pelagic fishes will also provide a baseline for comparison to fishes living in benthic or riverine environments.

Here we present the discovery of a mechanosensory lateral line canal within the bilateral keels of tunas with long tubules that extend to the upper and lower keel surfaces, accompanied by a suite of internal skeletal modifications associated with the lateral line canal. We further show that neuromast mechanoreceptor organs are found periodically along the canal. These observations suggest that the tuna keel acts as a flow sensing system, containing a canal that is substantially modified from the lateral line canal present along the body of other species of fishes.

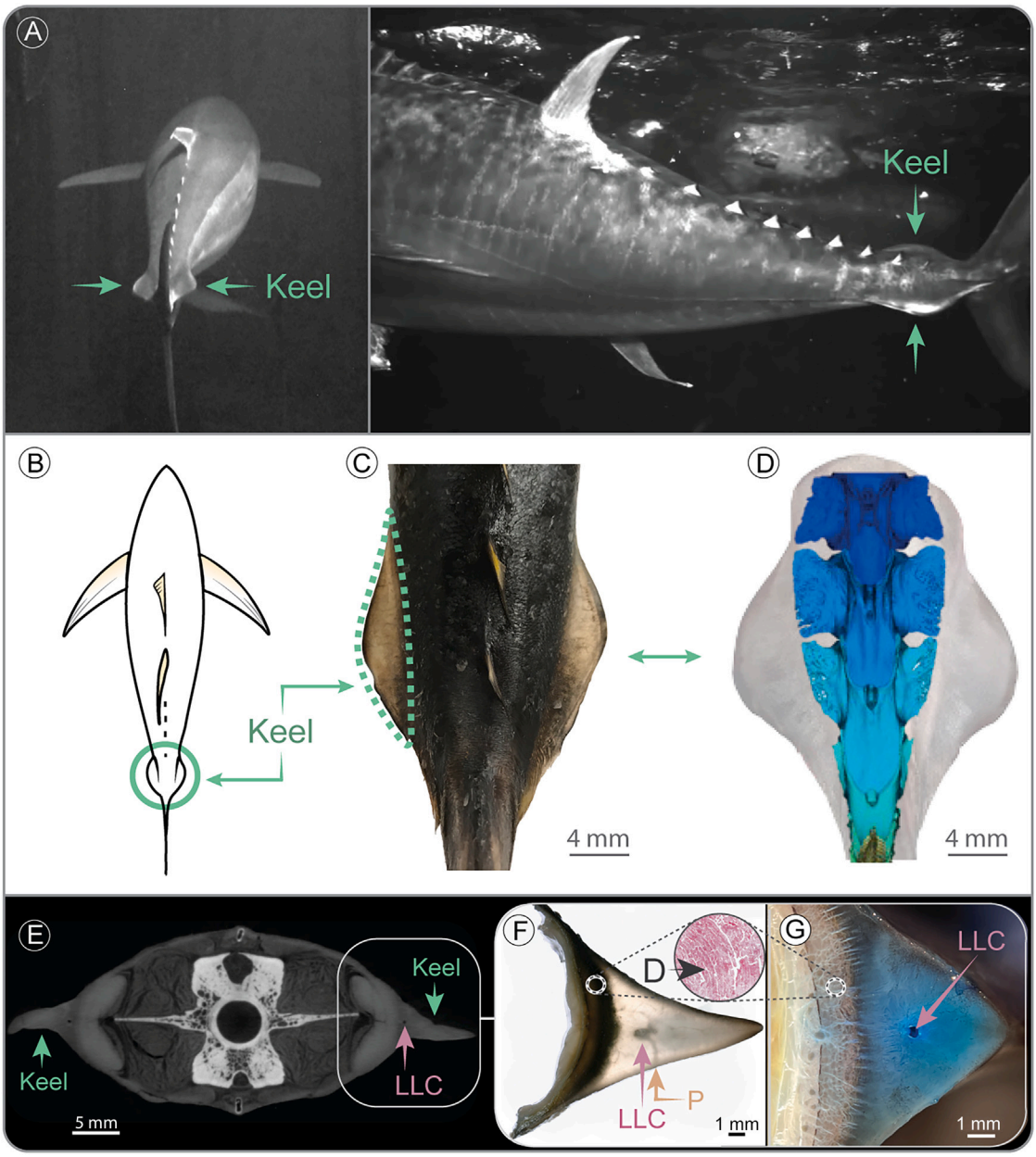


**Figure 1. Position and anatomy of the keel in tunas**

(A) Two frames from high-speed video of two individual yellowfin tuna (*Thunnus albacares*) swimming, showing the position of the lateral keels (green arrows) located on either side of the caudal peduncle, just rostral to the lunate tail. Tunas were approximately 1 m in length.

(B) Diagram showing dorsal view of a tuna, with the bilateral keels highlighted in green.

(C) Dorsal view of the peduncle, illustrating the shape of the keels.

(D) 3D reconstruction of the vertebral column in the caudal peduncle relative to the position of the soft keels. Note that the lateral expansions of the vertebrae and soft tissue keels are not aligned longitudinally.

(E) Cross-section of a PTA-stained specimen at the level of the caudal peduncle, showing the keels on both sides extending laterally from the lateral vertebral processes.

(F) Light microscopy cross-section showing the lateral line canal with a tubule extending to the keel surface and ending in a pore. Note the contrast between the fibrous tissue that forms the keel (translucent) and the density of the dermis medial to it. Inset: dermis stained with hematoxylin-eosin.

(G) Cross-section (hand cut) of the keel stained with methylene blue showing the cylindrical lateral line canal within the keel, and a neuromast in the medial wall of the canal. A fibrous network connects the keel tissue with additional fibrous connective tissue medial to it. Abbreviations: D, dermis; LLC, lateral line canal; P, pore.

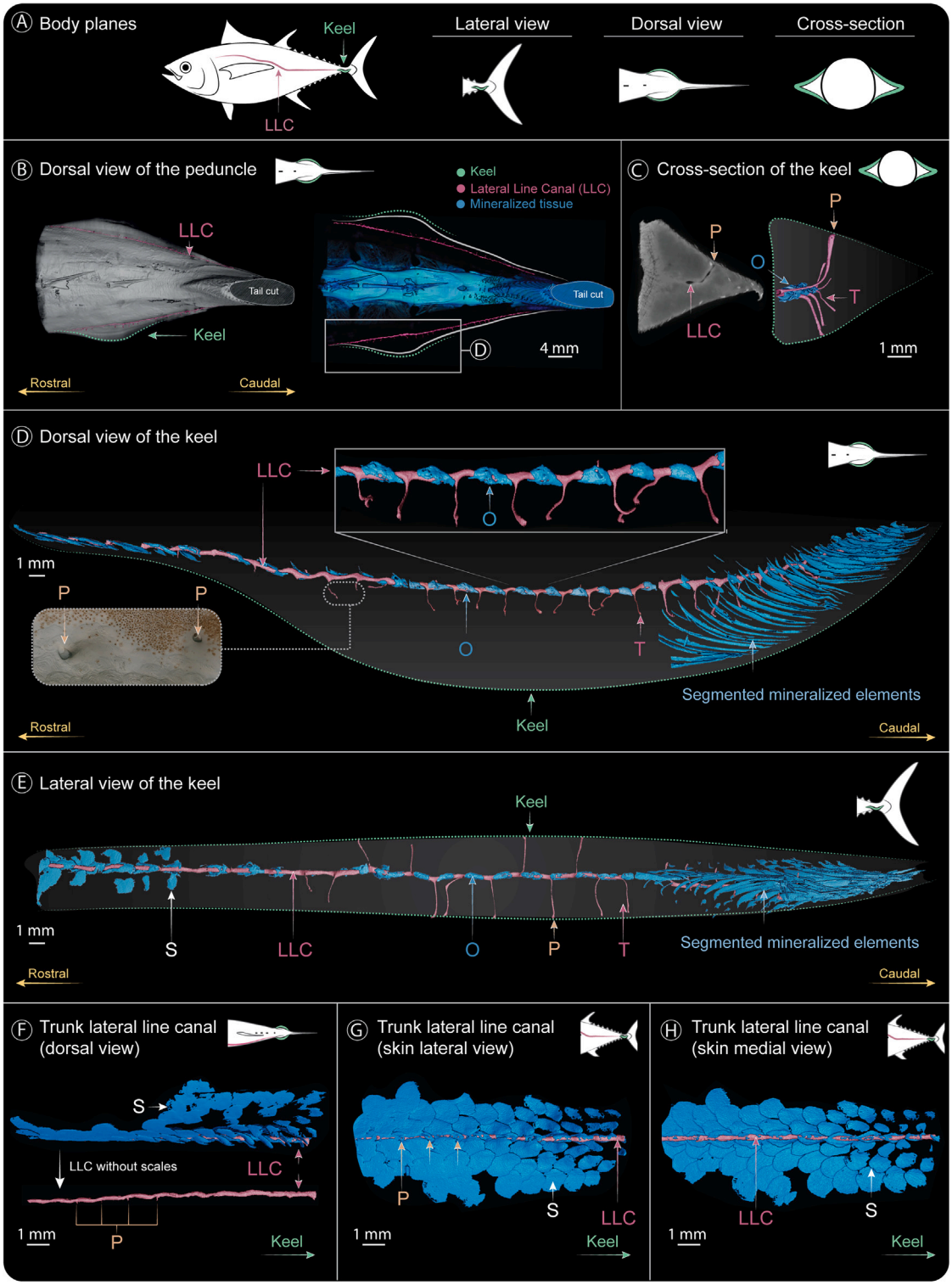


**Figure 2. Structure and anatomy of the lateral line canal in the tuna keel**

(A) Lateral, dorsal, and cross-sectional planes in tuna, showing the location of the keel (green) and the lateral line canal (pink).

(B) PTA-stained sample of the posterior part of the body of *Thunnus obesus* showing the keels on both sides of the caudal peduncle (lined in green) and the lateral line canal and tubules (pink). The image on the left shows the body with the skin. The image on the right shows the mineralized parts (vertebral column, in blue) and the lateral line canal.

*(legend continued on next page)*

## RESULTS

### Tuna keel structure

In this study, we morphologically characterized the keel region of two tuna species: *Thunnus albacares* (yellowfin) and *Thunnus obesus* (bigeye) using a combination of imaging techniques. Micro-computed tomography of samples stained with phosphotungstic acid was used to visualize the soft tissues of the lateral line canal in the tuna keels and trunk, as well as histological staining to visualize neuromasts within the canal. In these species of tunas, bilateral keels are located laterally on both sides of the caudal peduncle and extend caudally to the anterior limit of the lunate tail (Figures 1A–1D). We found that the keels are flexible structures formed by a collagenous matrix that is devoid of intrinsic muscle tissue (Figures 1E–1G). The collagenous matrix is anchored with fibrils to a thick dermis and, at the surface, the keels are covered by plate-like scales (Figures 1E–1G). Each keel contains a cylindrical lateral line canal that runs rostro-caudally, which we describe as a posterior extension of the lateral line trunk canal on the body (Figure 1G).

### The keel contains a lateral line canal with elongated tubules extending to the surface

Tunas are characterized by the presence of a sensory lateral line canal in the trunk that extends, along both sides of the body, from the head to the caudal peduncle (Figure 2, Videos S3, S4, and S5). On the trunk, the lateral line canal of tunas exhibits a similar morphology to that in other fishes[31,32] (Figures 2A and 2F–2H) consisting of a canal embedded within the lateral line scales near the body surface with pores perforating the scales and opening to the surrounding water (Figures 2F–2H).

In each lateral keel, the lateral line canal runs longitudinally and ends at the base of the lunate tail (Figures 2A and 2B). As the canal enters the keel, it undergoes a series of structural modifications that make it substantially different from the trunk canal in other parts in other parts of the tuna body, as well as from lateral line structures described previously in other fish species. Within the keel, the canal is lined by a smooth epithelium and it is embedded in the collagenous matrix well below the keel surface (Figures 1G and 2B–2E). A series of primary tubules extend from the lateral line canal both dorsally and ventrally at an angle of ~45° (Figures 2C–2E) through the keel's collagenous matrix until they reach the surface (Figures 2C–E). At the surface, each tubule opens through a pore connecting the lateral line canal to the surrounding fluid environment, resulting in a spatial distribution of pores that is linearly organized on both surfaces (Figures 2D and 2E; Videos S3, S4, and S5). The way in which tubules extend to the dorsal and ventral surfaces does not follow a pattern, although both surfaces have a similar number of pores. Within the keel, the lateral line canal, tubules and pores are distinct in diameter. Lateral line canals (diameter = 482.7 ± 7.9 μm in *Thunnus obesus*, and 371.8 ± 31.6 μm in *Thunnus albacares*, Table 1) are approximately 2.3 times larger in diameter than the tubules (tubule diameter = 181.9 ± 0.9 μm in *Thunnus obesus,* with a canal:tubule ratio of 2.6:1, and tubule diameter = 171.3 ± 15.1 μm in *Thunnus albacares*, with a tubule:canal ratio of 2.1:1; Table 1). The tubules are about 3 times larger in diameter than the pores (pore diameter = 137.7 ± 34.3 μm in *Thunnus obesus*, with a canal:pore ratio of 3.5:1, and pore diameter = 123.4 ± 4.24 μm in *Thunnus albacares*, with a canal:pore ratio of 3:1; Table 1).

The lateral line canal within the bilateral keels is surrounded at regular intervals by cylindrical mineralized structures composed of bone (Figures 2D–2E; Video S4). These ossifications appear to be plate-like scales that gradually encase the lateral line canal as it enters the keel (Figures 2D–2H). Upon entering the keel, these ossifications appear as isolated (non-overlaping) mineralized structures periodically positioned between tubules emerging from the canal (Figures 2D–2E; Video S3). This periodic pattern is maintained toward the posterior end of the keel, where the keel is supported by a skeletal framework composed of a group of thin, elongate, segmentally mineralized elements (Figures 2D and 2E; Video S5). The lateral line canal passes through this skeletal framework and terminates as it reaches the anterior end of the lunate tail without extending onto the tail itself (Figures 2A and 2B).

### The lateral line canal in the keel contains neuromasts surrounded by modified scales

We identified neuromasts within the lateral line canal, but they are absent in the tubules (Figure 3). Each neuromast is found within a cylindrical ossified element (described previously) and periodically distributed between adjacent tubules (Figure 3A). The neuromasts, which may be elongate (>90 μm long), are composed of sensory hair cells and supporting cells (Figures 3B and 3C). The globular structures observed above the neuromast in some histological sections (Figures 3B and 3C) likely correspond to structural remnants of hair cell death or remnants of the cupula (the gelatinous structure into which

(C) Cross-section of keel (right) showing the lateral line canal and emerging tubules (pink), showing one extending to the surface as a pore.
(D) Dorsal view of a 3D reconstruction of the lateral line system of the keel (rostral to right) illustrating the lateral line canal, the periodic mineralized cylindrical structures that surround the neuromasts (blue), tubules, and pores. Note how the plate-like scales gradually undergo modification caudally until they form independent (non-overlapping) ossifications located between adjacent tubules that emerge between them. There is a notable series of segmented mineralized elements within the posterior region of the keel shown to the right in blue, and the keel lateral line canal passes through these structures. The inset on the left shows the pores emerging onto the surface of the keel.
(E) Lateral view of the keel, showing how the tubules connect the lateral line canal to its dorsal and ventral surfaces. Note the plate-like scales and their transition to form the periodic cylindrical ossifications that surround the lateral line canal in the keel.
(F) Dorsal view of the lateral line canal (pink) in the trunk, rostral to the keel, showing the lateral line canal embedded within the scales (above) and the lateral line canal without scales (below) to clearly visualize the canal and pores. Note how the trunk lateral line canal lacks elongated tubules.
(G) Lateral view of the trunk lateral line canal (pink) showing the canal embedded in overlapping scales (blue) and how the pores perforate the scales. Plate-like scales are lost as the lateral line canal enters the keel on the right (caudal) in this image.
(H) Medial view (from inside the body) of the trunk lateral line canal. Note how the lateral line canal is progressively embedded within scales that take the form of periodic mineralized structures surrounding the canal as it enters the keel. Abbreviations: LLC, lateral line canal; O, ossifications; P, pores; S, scales; T, tubules.

**Table 1. Lateral line canal morphometrics**

| Species | Common name | SL (cm) | LLC diameter (μm) | | | Tubule diameter (μm) | | | Pore diameter (μm) | | | Canal: pore ratio | Ecology | Reference |
|---|---|---|---|---|---|---|---|---|---|---|---|---|---|---|
| | | | Min | Mean ± SD | Max | Min | Mean ± SD | Max | Min | Mean ± SD | Max | | | |
| *Thunnus obesus* | Big eye tuna | 152 | 388 | 488 ± 50.1 | 575 | 137 | 182 ± 37.7 | 236 | 146 | 161 ± 10.6 | 171 | 3:1 | Marine/ pelagic | This study |
| *Thunnus obesus* | Big eye tuna | 133 | 234 | 477 ± 150.3 | 818 | 70 | 181 ± 54.8 | 259 | 75 | 113 ± 29.3 | 154 | 4:1 | Marine/ pelagic | This study |
| *Thunnus albacares* | Yellowfin tuna | 103 | 153 | 349 ± 88.7 | 518 | 93 | 160 ± 42.4 | 270 | 14 | 126 ± 59.8 | 226 | 3:1 | Marine/ pelagic | This study |
| *Thunnus albacares* | Yellowfin tuna | 100 | 289 | 394 ± 49.2 | 479 | 140 | 182 ± 20.3 | 212 | 73 | 120 ± 36.2 | 167 | 3:1 | Marine/ pelagic | This study |
| *Cymatogaster aggregata* | Shiner perch | 7.5 | – | 222 | – | – | – | – | – | 20 | – | 11:1 | Marine/ demersal | Webb et al.[26] |
| *Abudefduf saxatilis* | Sergeant major | 6.5 | – | 237 | – | – | – | – | – | 268 | – | 1:1 | Marine/ coral reefs | Webb et al.[26] |
| *Amphiprion ocellaris* | Clown fish | 4.5 | – | 237 | – | – | – | – | – | 270 | – | 1:1 | Marine/ coral reefs | Webb et al.[26] |
| *Xiphister atropurpureus* | Black prickleback | 20 | – | 500 | – | – | – | – | – | 300 | – | 2:1 | Marine/ demersal | Bleckmann et al.[33] |
| *Hexagrammos decagrammus* | Kelp greenling | 22 | – | 360 | – | – | – | – | – | – | – | – | Marine/ benthic | Wonsettler et al.[34] |
| *Argyropelecus aculeatus* | Hatchetfish | 3.9 | – | 253 | – | – | – | – | – | – | – | – | Marine/ mesopelagic | Marranzino et al.[35] |
| *Tilapia nilotica* | Nile tilapia | 13 | – | 190 | – | – | – | – | – | – | – | – | Freshwater/ pelagic | Münz[36] |

Comparison of lateral line canal, tubules, and pores diameters and ratios in tuna keels and the lateral line canal, tubules, and pores in the trunk in a diversity of teleost fishes with different ecologies. Values are represented as mean with standard deviation, minimum and maximum values. Abb: SL (standard length).

the ciliary bundles of the sensory hair cells extend, which is generally lost in preparation for imaging) (Figures 3B). Blood vessels and nerve axons are clearly seen in cross-section below the neuromast tissue and penetrate the ossified elements within which the neuromasts are enclosed (Figure 3C).

## DISCUSSION

Tunas in the genus *Thunnus* are highly valued in global commercial fisheries, owing to their widespread demand in the seafood industry.[37] They are characterized by numerous morphological, physiological, and biomechanical adaptations for high-speed swimming and a pelagic lifestyle,[38] and are capable of migrating long distances and sustaining high-speed swimming for extended periods of time.[1,6,9,10,39,40] These adaptations are reflected in the tuna body structure, including a streamlined body shape to reduce drag, a lunate high-aspect caudal fin, cardiovascular specializations, specialized locomotor musculature and tendons,[41–43] a narrow caudal peduncle with finlets, and the presence of a bilateral keels along both sides of the caudal peduncle.[4,39,44]

Bilateral keels associated with the caudal fin (Figure 1) are present in several pelagic swimmers, evolving convergently in species such as lamnid sharks (e.g., white and mako sharks), billfishes, whale sharks, and cetaceans.[44–46] The limited previous research on the keels in fishes focuses on their biomechanical functions and suggests that keels streamline the peduncle during side-to-side motion and increase swimming efficiency by decreasing fluid turbulence, yaw torques, and drag around the caudal peduncle.[4,21] However, little is known about keel morphology and function beyond their role in locomotion.

We report here that each of the bilateral keels of two species of tunas contain a novel internal lateral line canal with numerous small tubules that extend to both the dorsal and ventral surface terminating in canal pores at the surface (Figure 2). We also demonstrate that the lateral line canal in each keel contains neuromast receptor organs within the lumen of the canal, surrounded by what are interpreted as modified lateral line scales (Figures 2 and 3). Furthermore, the posterior region of each keel is supported by a series of thin segmentally arranged skeletal elements of unknown homology and function that surrounds the lateral line canal in this region, which may be modified scales (Figure 2D and 2E).

The presence of a lateral line canal within the keel indicates that in addition to their biomechanical function, keels play a mechanosensory role enabling the detection of fluid motion at the keel surface. The lateral line canal within the keel is substantially different in morphology from the lateral line canal along the rest of the body and the lateral line canal described in other fishes.[26,31] The tubules that extend from the canal to the dorsal and ventral surfaces of the keel terminate in a well-defined series of pores linearly distributed along the dorsal and ventral surfaces of the keel (Figure 2E). In tunas, the surface of the keels is subjected to high-velocity flows, characterized by strong,

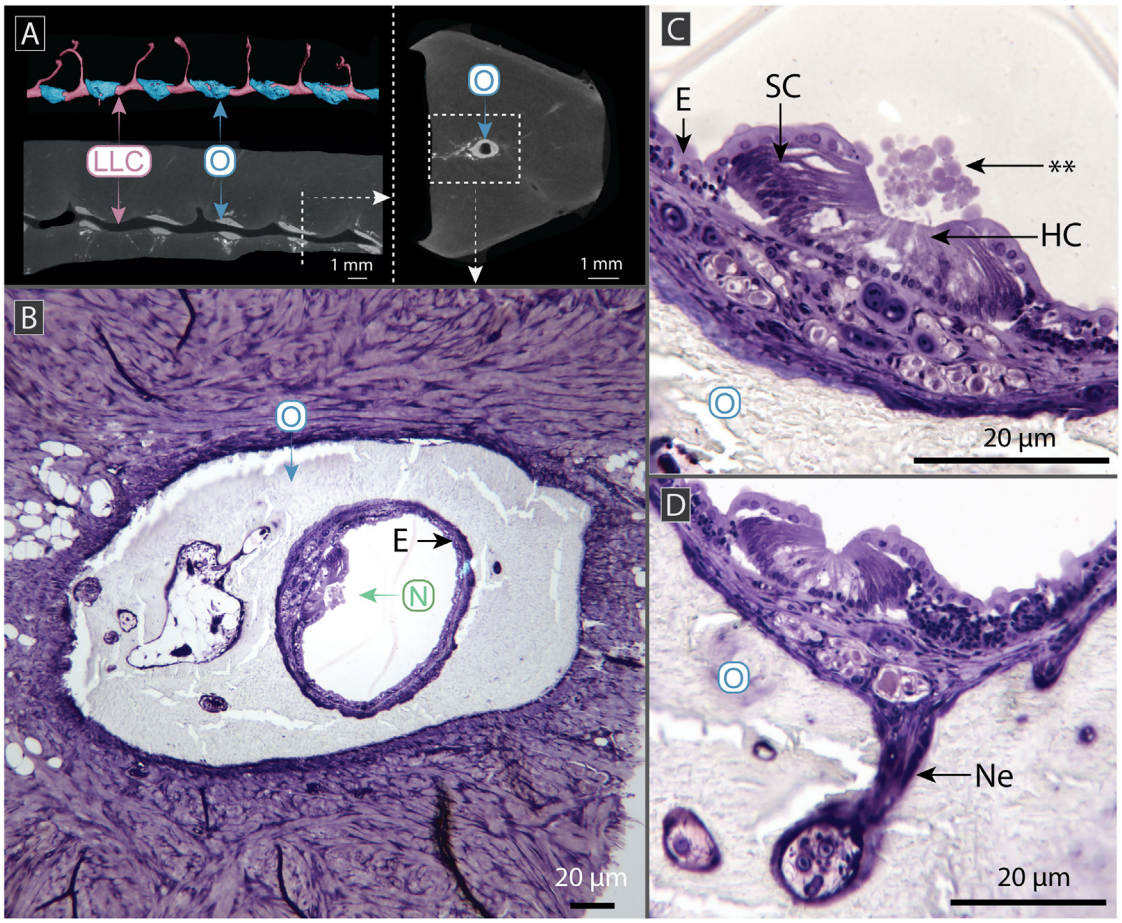


**Figure 3. Neuromast anatomy within the lateral line canal in the keel**

(A) Lateral line canal showing the periodic ossifications that surround the canal; neuromasts are only found within the segments of the canal surrounded by the ossifications. Cross-section of the lateral line canal and the ossifications in a PTA-stained specimen (bottom). Cross-section of a PTA-stained keel illustrating a single ossification surrounding the lateral line canal.

(B) Transverse section of cresyl violet stained tissue (see box in A) with a neuromast within the canal, surrounded by an ossification (unstained material). The canal lumen is lined by epithelial tissue, and the neuromast is located in the medial (proximal) wall of the canal.

(C) Transverse section of neuromast at higher magnification showing hair cells and the supporting cells. The globular structure is likely remnants of the gelatinous neurommast cupula that is typically lost during tissue preparation or an indication of hair cell death; blood vessels and neurons are present below the neuromast.

(D) Transverse section of neuromast showing a branch of the lateral line nerve traversing the ossified structure to innervate the neuromast. Abbreviations: E, epithelium lining canal; (**), globular structure; HC, hair cells; LLC, lateral line canal; N, neuromast; Ne, nerve; O, ossifications; SC, supporting cells.

high-frequency and high-amplitude, streamwise vortices that produce pressure differences across the keel surface during tail movement.[3,21] In addition, it has been shown that the keel region of the caudal peduncle in mackerel (a relative of tunas) is subject not only to streamwise flow but also to alternating circumferential flow around the peduncle due to the side-to-side motion of the tail during propulsion.[19] The position of the tubules and the linear array of surface pores in the tuna keel suggest that the lateral line canal is collecting information from both dorsal and ventral keel surfaces and should be able to detect differences in pressure along both surfaces.

The smaller diameter of tubules and pores relative to that of the canal, along with differences in number of tubule branches and spatial distribution of surface pores on the keel surface (Table 1), may determine stimulus filtering to reduce hydrodynamic noise generated by body movements and turbulence associated with peduncular flow dynamics. For example, these morphological characteristics may alter the magnitude and frequency response of fluid within the canal that activates the canal neuromasts.[28,47] Pores with a smaller diameter reduce the sensitivity of the neuromasts within the lateral line canal by increasing flow resistance within the tubule, as higher pressures need to be applied to produce a movement of the gel-like fluid within the canal that stimulates a neuromast.[47,48] However, a pressure drop generated by moving water along the keel surface will propagate over long distances within the lateral line canal, increasing the relative influence of each pore along the canal.[47] Therefore, the observed modifications of the lateral line system in the keel relative to the trunk canal of tunas and other fishes (Table 1) may be a result of the adaptation for sensing the hydrodynamic

environment of the tuna keel, where only flows able to generate high pressures may stimulate canal neuromasts. The viscosity of the fluid within the lateral line canal of tuna remains unknown, including whether the fluid in the keel canal differs from that in the trunk canal on the body or how it varies among species.

The presence of canal neuromasts surrounded by ossifications may reflect another adaptation to the high-frequency conditions of the keel environment. These ossifications appear to be modifications of tubed lateral line scales, as scales become reduced (losing the flat scale plate) as the canal enters the keel (Figure 2). Keel structures are subject to high-frequency (up to 15 Hz) oscillatory lateral motion during propulsion.[3,4,15,23] The retention of these cylindrical ossifications may function to protect and stabilize the neuromasts, as well as the nerve entering each neuromast, due to the potential for deformation as a result of the rapid and high-amplitude movement in the region of the caudal peduncle during tuna propulsion and maneuvering (Videos S1 and S2).

Quantitative comparisons among data on the lateral line canal of the tuna keel and lateral line canals in other fishes are challenging due to the scarcity of published data on the lateral line canal, and the tubules and pore diameters in other fish species. A further complication is the large body size of the tunas studied here and previous analyses of lateral line structure in other fishes, which are generally less than 20 cm total length. Nevertheless, Table 1 presents a selection of canal metrics from this study and values measured from published figures on other species, along with fish body length estimates, where available. We show that the diameter of the lateral line canal in tuna keels is 1–2 times larger than the canal diameter in other fish species, while surface pore diameters are generally half of the diameter of pores in other species (with the exception of the shiner perch that appear to have very small surface pores on the order of 20 μm). We were unable to locate published data from other species on the diameter of tubules that connect the lateral line canal to surface pores but, in the tuna keel, tubules are approximately half the diameter of the canal (Table 1).

We propose here that the lateral line canal in the keel of tunas acts as a mechanosensory structure. The mechanosensory function of the bilateral keels of tunas adds to the impressive suite of structural adaptations for high-speed locomotion and a pelagic lifestyle that define tunas as apex oceanic predators.

### Limitations of the study

In this study we have focused on two species of tuna, but a much wider comparative study would be valuable to determine if a modified lateral line canal is found in other species with keels, including other tunas but also species such as whale sharks, mackerels, and billfishes. Keel-like structures vary considerably among pelagic fish species, and a specialized lateral line canal within the keel could be a more general feature of high-speed pelagic fishes. Due to the many challenges in obtaining samples from tuna that could be used for laboratory physiological analysis, conducting functional physiological studies on the lateral line of tunas is not currently feasible to experimentally analyze how signals from the ambient fluid environment are transmitted to the central nervous system.

## RESOURCE AVAILABILITY

### Lead contact

Requests for further information and resources should be directed to and will be fulfilled by the lead contact, Júlia Chaumel (julia_chaumelcerda@fas.harvard.edu).

### Materials availability

This study did not generate new unique reagents.

### Data and code availability

- Original histology images and raw CT scan images used for the 3D reconstructions have been deposited at Mendeley Data repository and are publicly available as of the date of publication. Accession numbers are listed in the key resources table.
- This paper does not report original code.
- Any additional information required to reanalyze the data reported in this paper is available from the lead contact upon request.

## ACKNOWLEDGMENTS

Many thanks to members of the Lauder Lab for their assistance with this project and to Andy Williston and Meaghan Sorce in the Fish Department of the MCZ. The Lauder Lab also expresses their appreciation to Greenfins Inc. and especially to T. Bradley and P. Mottur for allowing us access and providing assistance in obtaining high-speed video of tuna swimming in their facility.

This research was funded by the Deutsche Forschungsgemeinschaft project number (510759809) to J.C., by the Office of Naval Research grants N000141410533 and N00014-15-1-2234 to G.V.L., and the George and Barbara Young Chair in Biology at University of Rhode Island to J.F.W. This study was published by a grant from the Wetmore Colles fund.

## AUTHOR CONTRIBUTIONS

Initial conceptualization: D.K.W., C.F.W., and G.V.L.; methodology and data acquisition: J.C., J.F.W., C.F.W., and D.K.W.; data analysis: J.C. and J.F.W.; writing – original draft: J.C. and G.V.L.; writing – editing and manuscript revisions: D.K.W., C.F.W., G.V.L., J.F.W., and J.C.; visualization: J.C. and J.F.W.; funding acquisition: J.C. and G.V.L. All authors gave final approval for publication and agree to be held accountable for the work described herein.

## DECLARATION OF INTERESTS

The authors declare no competing interests.

## DECLARATION OF GENERATIVE AI AND AI-ASSITANCE TECHNOLOGIES IN THE WRITING PROCESS

During the preparation of this work the authors did not use any AI and/or AI-assistance technologies.

## STAR★METHODS

Detailed methods are provided in the online version of this paper and include the following:

- KEY RESOURCES TABLE
- EXPERIMENTAL MODEL AND STUDY PARTICIPANT DETAILS
- METHOD DETAILS
  - Histology and light microscopy
  - Micro computed tomography (μCT scan)
  - 3D segmentation and analysis
  - Video data
- QUANTIFICATION AND STATISTICAL ANALYSIS

## SUPPLEMENTAL INFORMATION

Supplemental information can be found online at https://doi.org/10.1016/j.isci.2024.111578.

Received: August 12, 2024
Revised: October 9, 2024
Accepted: December 9, 2024
Published: December 12, 2024

## REFERENCES

1. Block, B.A., and Stevens, E.D. (2001). Tuna: Physiology, Ecology, and Evolution (Gulf Professional Publishing).
2. Shadwick, R. (2005). How Tunas and Lamnid Sharks Swim: An Evolutionary Covergence: These fishes diverged millions of years ago, but selection presures have brought them very similar biomechanical schemes for movement. Am. Sci. *93*, 524–531.
3. Zhu, J., White, C., Wainwright, D.K., Di Santo, V., Lauder, G.V., and Bart-Smith, H. (2019). Tuna robotics: A high-frequency experimental platform exploring the performance space of swimming fishes. Sci. Robot. *4*, eaax4615.
4. Wainwright, D.K., and Lauder, G.V. (2020). Tunas as a high-performance fish platform for inspiring the next generation of autonomous underwater vehicles. Bioinspir. Biomim. *15*, 035007.
5. Lutcavage, M.E., Brill, R.W., Skomal, G.B., Chase, B.C., Goldstein, J.L., and Tutein, J. (2000). Tracking adult North Atlantic bluefin tuna (Thunnus thynnus) in the northwestern Atlantic using ultrasonic telemetry. Mar. Biol. *137*, 347–358.
6. Block, B.A., Teo, S.L.H., Walli, A., Boustany, A., Stokesbury, M.J.W., Farwell, C.J., Weng, K.C., Dewar, H., and Williams, T.D. (2005). Electronic tagging and population structure of Atlantic bluefin tuna. Nature *434*, 1121–1127.
7. Wilson, S.G., Lutcavage, M.E., Brill, R.W., Genovese, M.P., Cooper, A.B., and Everly, A.W. (2005). Movements of bluefin tuna (Thunnus thynnus) in the northwestern Atlantic Ocean recorded by pop-up satellite archival tags. Mar. Biol. *146*, 409–423.
8. Madigan, D.J., Baumann, Z., and Fisher, N.S. (2012). Pacific bluefin tuna transport Fukushima-derived radionuclides from Japan to California. Proc. Natl. Acad. Sci. USA *109*, 9483–9486.
9. Collette, B., Graves, J., and Kells, V.A. (2019). Tunas and Billfishes of the World (Johns Hopkins University Press).
10. Gleiss, A.C., Schallert, R.J., Dale, J.J., Wilson, S.G., and Block, B.A. (2019). Direct measurement of swimming and diving kinematics of giant Atlantic bluefin tuna (*Thunnus thynnus*). R. Soc. Open Sci. *6*, 190203.
11. Downs, A.M., Kolpas, A., Block, B.A., and Fish, F.E. (2023). Multiple behaviors for turning performance of Pacific bluefin tuna (Thunnus orientalis). J. Exp. Biol. *226*, jeb244144.
12. Takagi, T., Tamura, Y., and Weihs, D. (2013). Hydrodynamics and energy-saving swimming techniques of Pacific bluefin tuna. J. Theor. Biol. *336*, 158–172.
13. Newlands, N.K., and Porcelli, T.A. (2008). Measurement of the size, shape and structure of Atlantic bluefin tuna schools in the open ocean. Fish. Res. *91*, 42–55.
14. Thandiackal, R., White, C.H., Bart-Smith, H., and Lauder, G.V. (2021). Tuna robotics: hydrodynamics of rapid linear accelerations. Proc. Biol. Sci. *288*, 20202726.
15. White, C.H., Lauder, G.V., and Bart-Smith, H. (2021). Tunabot Flex: A tuna-inspired robot with body flexibility improves high-performance swimming. Bioinspir. Biomim. *16*, 026019.
16. Bushnell, P.G., and Jones, D.R. (1994). Cardiovascular and respiratory physiology of tuna: adaptations for support of exceptionally high metabolic rates. Environ. Biol. Fish. *40*, 303–318.
17. Brill, R.W., and Bushnell, P.G. (2001). The cardiovascular system of tunas. Fish Physiol. *19*, 79–120.
18. Graham, J.B., and Dickson, K.A. (2004). Tuna comparative physiology. J. Exp. Biol. *207*, 4015–4024.
19. Nauen, J.C., and Lauder, G.V. (2000). Locomotion in scombrid fishes: morphology and kinematics of the finlets of the chub mackerel Scomber japonicus. J. Exp. Biol. *203*, 2247–2259.
20. Shadwick, R.E., and Syme, D.A. (2008). Thunniform swimming: muscle dynamics and mechanical power production of aerobic fibres in yellowfin tuna (Thunnus albacares). J. Exp. Biol. *211*, 1603–1611.
21. Zhang, J.-D., Sung, H.J., and Huang, W.-X. (2020). Specialization of tuna: A numerical study on the function of caudal keels. Phys. Fluids *32*, 11.
22. Wang, J., Wainwright, D.K., Lindengren, R.E., Lauder, G.V., and Dong, H. (2020). Tuna locomotion: a computational hydrodynamic analysis of finlet function. J. R. Soc. Interface *17*, 20190590.
23. Donley, J.M., and Dickson, K.A. (2000). Swimming kinematics of juvenile kawakawa tuna (Euthynnus affinis) and chub mackerel (Scomber japonicus). J. Exp. Biol. *203*, 3103–3116.
24. Di Santo, V., Goerig, E., Wainwright, D.K., Akanyeti, O., Liao, J.C., Castro-Santos, T., and Lauder, G.V. (2021). Convergence of undulatory swimming kinematics across a diversity of fishes. Proc. Natl. Acad. Sci. USA *118*, e2113206118.
25. Bleckmann, H., and Zelick, R. (2009). Lateral line system of fish. Integr. Zool. *4*, 13–25.
26. Webb, J.F., and Ramsay, J.B. (2017). New interpretation of the 3-D configuration of lateral line scales and the lateral line canal contained within them. Copeia *105*, 339–347.
27. Van Netten, S.M. (2006). Hydrodynamic detection by cupulae in a lateral line canal: functional relations between physics and physiology. Biol. Cybern. *94*, 67–85.
28. van Netten, S.M., and McHenry, M.J. (2014). The biophysics of the fish lateral line. In The lateral line system, S. Coombs, H. Bleckmann, R.R. Fay, and A.N. Popper, eds. (Heidelberg, Germany: Springer), pp. 99–119.
29. Coombs, S., Görner, P., and Münz, H. (2012). The Mechanosensory Lateral Line: Neurobiology and Evolution (Springer Science & Business Media).
30. Jordan, L.K., Kajiura, S.M., and Gordon, M.S. (2009). Functional consequences of structural differences in stingray sensory systems. Part I: mechanosensory lateral line canals. J. Exp. Biol. *212*, 3037–3043.
31. Webb, J.F. (2014). Lateral line morphology and development and implications for the ontogeny of flow sensing in fishes. In Flow sensing in air and water: Behavioral, neural and engineering principles of operation (Springer), pp. 247–270.
32. Webb, J.F. (2014). Morphological diversity, development, and evolution of the mechanosensory lateral line. In The lateral line system, S. Coombs, H. Bleckmann, R.R. Fay, and A.N. Popper, eds. (Heidelberg, Germany: Springer), pp. 17–72.
33. Bleckmann, H., and Münz, H. (1990). Physiology of lateral-line mechanoreceptors in a teleost with highly branched, multiple lateral lines. Brain Behav. Evol. *35*, 240–250.
34. Wonsettler, A.L., and Webb, J.F. (1997). Morphology and development of the multiple lateral line canals on the trunk in two species of Hexagrammos (Scorpaeniformes, Hexagrammidae). J. Morphol. *233*, 195–214.
35. Marranzino, A.N., and Webb, J.F. (2018). Flow sensing in the deep sea: the lateral line system of stomiiform fishes. Zool. J. Linn. Soc. *183*, 945–965.
36. Münz, H. (1979). Morphology and innervation of the lateral line system in Sarotherodon niloticus (L.)(Cichlidae, Teleostei). Zoomorphologie *93*, 73–86.
37. Coit, J. (2021). Improving International Fisheries Management: 2023 Report to Congress (National Oceanic and Atmospheric Administration).
38. Bernal, D., Sepulveda, C., Musyl, M., and Brill, R. (2009). The eco-physiology of swimming and movement patterns of tunas, billfishes, and large

pelagic sharks. In Fish locomotion—an etho-ecological approach (Enfield, NH: Enfield Scientific Publishers), pp. 437–483.

39. Shadwick, R.E., and Goldbogen, J.A. (2012). Muscle function and swimming in sharks. J. Fish. Biol. *80*, 1904–1939.
40. Bernal, D., Brill, R.W., Dickson, K.A., and Shiels, H.A. (2017). Sharing the water column: physiological mechanisms underlying species-specific habitat use in tunas. Rev. Fish Biol. Fish. *27*, 843–880.
41. George, J.C., and Don Stevens, E. (1978). Fine structure and metabolic adaptation of red and white muscles in tuna. Environ. Biol. Fish. *3*, 185–191.
42. Sharp, G. (2012). The Physiological Ecology of Tunas (Elsevier).
43. Nakae, M., Sasaki, K., Shinohara, G., Okada, T., and Matsuura, K. (2014). Muscular system in the pacific bluefin tuna Thunnus orientalis (Teleostei: Scombridae). J. Morphol. *275*, 217–229.
44. Bernal, D., Dickson, K.A., Shadwick, R.E., and Graham, J.B. (2001). Analysis of the evolutionary convergence for high performance swimming in lamnid sharks and tunas. Comp. Biochem. Physiol. Mol. Integr. Physiol. *129*, 695–726.
45. Hill, D.K. (1986). Age and growth of the Pacific blue marlin, Makaira nigricans: a comparison of growth zones in otoliths, vertebrae, and dorsal and anal spines. Master's thesis (California State University, Stanislaus).
46. Hamilton, J.L., Dillaman, R.M., McLellan, W.A., and Pabst, D.A. (2004). Structural fiber reinforcement of keel blubber in harbor porpoise (Phocoena phocoena). J. Morphol. *261*, 105–117.
47. Klein, A., and Bleckmann, H. (2015). Function of lateral line canal morphology. Integr. Zool. *10*, 111–121.
48. Klein, A., Münz, H., and Bleckmann, H. (2013). The functional significance of lateral line canal morphology on the trunk of the marine teleost Xiphister atropurpureus (Stichaeidae). J. Comp. Physiol. *199*, 735–749.
49. Metscher, B.D. (2009). MicroCT for comparative morphology: simple staining methods allow high-contrast 3D imaging of diverse non-mineralized animal tissues. BMC Physiol. *9*, 11–14.

## STAR★METHODS

### KEY RESOURCES TABLE

| REAGENT or RESOURCE | SOURCE | IDENTIFIER |
|---|---|---|
| Biological samples | | |
| *Thunnus albacares* (n=3) | Northwest Atlantic | N/A |
| *Thunnus obesus* (n=2) | Northwest Atlantic | N/A |
| Chemicals, peptides, and recombinant proteins | | |
| Glycol methacrylate resin | Kulzer Technik | Technovit 7100 |
| 10% neutral buffered formalin | VWR | 89370-094 |
| Phosphotungstic acid | AMRESCO | 0371-100G |
| Iodine | Fisher Scientific | 934412 |
| Methylene blue | Allied Chemical | 0652 |
| Cresyl violet | Millipore Sigma | 105010-54-0 |
| Epredia Decalcifying Solution | Fisher Scientific | 72060-100 |
| Mayer's hematoxylin solution | Sigma Aldrich | MHS16-500ML |
| Eosin Y solution | Sigma Aldrich | 318906-500ML |
| Deposited data | | |
| Micro-computed tomography raw data sets | Mendeley Data | https://doi.org/10.17632/c3sr6w3ywf.1 |
| Original histology images | This paper; Mendeley Data | https://doi.org/10.17632/c3sr6w3ywf.1 |
| Original keel surface images | This paper; Mendeley Data | https://doi.org/10.17632/c3sr6w3ywf.1 |
| Software and algorithms | | |
| Amira Avizo Software | ThermoFisher | Version 2023.11 |
| Bruker Skyscan | Bruker | 1273 |
| Keyence digital microscope | Keyence Corporation | VHX-600 |
| Other | | |
| Photron Mini AX100 camera | Photron | N/A |

### EXPERIMENTAL MODEL AND STUDY PARTICIPANT DETAILS

This study used the keels of a total of 5 adult individuals from two species of tuna; two *Thunnus obesus* (bigeye tuna) and three *Thunnus albacares* (yellowfin tuna). All individuals were captured in the northwest Atlantic in the area surrounding Atlantis Canyon (39.87°, −70.25°). *Thunnus obesus* ($n = 2$, fork lengths = 140 & 160 cm) were captured on August 12, 2020. *Thunnus albacares* were captured on July 24$^{th}$, 2020 ($n = 2$, FL = 107 & 140 cm) and August 12$^{th}$, 2020 ($n = 1$, FL = 104 cm). Gender was not determined for any individuals. Animals were collected under permit number HMS-SRP-19-03.

Video data of captive *T. albacares* were obtained at the Greenfins Inc. tuna facility (University of Rhode Island, Narragansett, RI, USA) as fish swam freely in a 473,000-L, saltwater, circular tank (12.2 m in diameter, >3 m depth). As fish were not captured, gender and length of individuals are not known. However, the fish were approximately 1 m in length. This procedure was conducted in accordance with approved animal protocol IACUC 20-03-4 by Harvard University.

### METHOD DETAILS

Tunas were captured on rod and reel tackle in the Northwest Atlantic, in the vicinity of Atlantis Canyon. Shortly after capture, keels were removed and fixed in 10% neutral buffered formalin. Samples from one keel from *Thunnus albacares* (FL = 104 cm, fork length) was used for histology; the other keel from the same individual *T. albacares*, a keel from *T. albacares* (FL = 107 cm), a keel from *Thunnus obesus* (FL = 140 cm), and a keel from *T. obesus* (FL = 160 cm) were PTA-stained and scanned using micro-computed tomography (μCT). A whole peduncle of a *T. albacares* was also scanned and, although the FL was unknown, it could be estimated to be < 100 cm.

#### Histology and light microscopy

A weak solution of methylene blue (Allied Chemical) was used to reveal the longitudinal canal and surrounding connective tissues in the keel of *T. obesus* that had been removed from the body. The lateral line canal in the keel of one *T. albacares* (104 cm FL) was

dissected for histological staining. For hematoxylin and eosin staining, sections were decalcified with Epredia Decalcifying Solution (Fisher Scientific) for 48 h and dehydrated using an ascending series of ethanol solutions (50%, 70%, 85% and 100%). Samples were then transferred to 100% xylene, embedded in paraffin, sectioned at 5μm thickness, mounted, and stained with hematoxylin-eosin (Sigma Aldrich). For cresyl violet staining, tissues were dehydrated in an ascending series of ethanol solutions (50%, 70%, 85%, 95%) and embedded in glycol methacrylate resin (Technovit 7100; Kulzer Technik). Tissues were sectioned at 5μm thickness (every 2nd section was mounted on glass slide, yielding a 10μm section interval), and air dried overnight. Slides were stained with 0.5% cresyl violet (Millipore Sigma) rinsed in running tap water, air dried and coverslipped (Entellan, Electron Microscopy Sciences). Tissues were imaged on Olympus BH-2 compound microscope. Images of the keel cross-section and the surface were acquired using a Keyence digital microscope VHX-600 (Keyence Corporation).

### Micro computed tomography (μCT scan)

Tuna peduncle and keels of two *T. albacares* (104 cm and 107 cm FL) and of two *T. obesus* (140 cm and 160 cm FL) were imaged using micro computed tomography (μCT scanning) on a Brucker Skyscan 1273 (Bruker). Prior to scanning, samples fixed in 10% formalin were washed in phosphate buffered saline (PBS; 3 times 5 min each) and then dehydrated in increasing ethanol concentrations (up to 70% ethanol). For scanning, samples were placed in plastic vials, surrounded with cheese cloth moisturized with ethanol 70%, ethanol to avoid desiccation. After being scanned, samples were stained with different contrasting agents to increase the contrast of soft tissues and make them visible using X-rays. Due to the rapid penetration of iodine,[49] the peduncle and a sample from the anterior part of the body anterior to the keel were stained in 1% iodine (Fisher Scientific) during one week in 100% ethanol and μCT scanned. The peduncle was scanned at 44 μm pixel size, with a voltage of 166 μA, and a current of 90 kV. The anterior body sample was μCT scanned at 7.9 μm pixel size, with a voltage of 100 μA, and a current of 80 kV. Keels were cut into small pieces (1 cm thickness), stained with 1% phosphotungstic acid (PTA, AMRESCO) in 70% ethanol for several months, and μCT scanned. PTA was used due to its optimal results in staining fish soft tissues.[49] A voltage of 187 μA and a current of 80 kV were used for all scans, but image pixel size ranged between 15 and 20 μm based on the size of the samples.

### 3D segmentation and analysis

Raw image datasets obtained with the μCT scan were reconstructed using Bruker Skyscan 1273 software (Bruker). Once reconstructed, image datasets were rendered, segmented and measured using Amira-Avizo visualization software (version 2023.11, ThermoFisher). Lateral line measurements included the diameter of the lateral line canals, tubules, and pores. Measures of the lateral line diameter of other fish species were collected using previously published images.

### Video data

High-speed videos of swimming kinematics of yellowfin tuna (*Thunnus albacares*) were obtained to show the position of the caudal keels during active locomotion (Figure 1; Videos S1 and S2) following the procedures described in.[3] Briefly, video data were obtained at the Greenfins Inc. tuna facility (University of Rhode Island, Narragansett, RI, USA) where tuna averaging 1 m in length swam freely in a 473,000-L, saltwater, circular tank (12.2 m in diameter, >3 m depth) in which locomotion is largely unconstrained; fish are free to change direction and maneuver. A Photron Mini AX100 camera at 250 and 500 fps was used. Video frames in Figure 1 were obtained from feeding sequences where tunas were actively feeding and maneuvering to capture immobile mackerel and squid prey.

## QUANTIFICATION AND STATISTICAL ANALYSIS

Measurements of tubule curvature and the diameters of canals, tubules, and pores in the lateral line system of tuna keels were performed using Amira Avizo Software (version 2023.11, ThermoFisher). For comparison, the diameters of lateral line canals, tubules, and pores in other fish species were directly extracted from published images. These measurements can be found in Table 1.